Infinitely Many Knots With NonIntegral Trace

A. W. Reid & N. Rouse

Published online: 15 Oct 2021.

Submit your article to this journal ↗

View related articles ↗

View Crossmark data ↗

Taylor & Francis
Taylor & Francis Group

Check for updates

Infinitely Many Knots With NonIntegral Trace

A. W. Reid and N. Rouse

Department of Mathematics, Rice University, Houston, TX, USA

ABSTRACT
We prove that there are infinitely many non-homeomorphic hyperbolic knot complements $S^3 \setminus K_i = \mathbb{H}^3 / \Gamma_i$ for which Γ_i contains elements whose trace is an algebraic non-integer.

1. Introduction

A basic consequence of Mostow-Prasad Rigidity is that if $M = \mathbb{H}^3 / \Gamma$ is an orientable hyperbolic 3-manifold of finite volume, then the traces of the elements in Γ are algebraic numbers (see [19, Theorem 3.1.2]). In addition, if there is an element $\gamma \in \Gamma$ for which the trace is an algebraic *non-integer*, then Bass's Theorem [3] implies that M contains a closed embedded essential surface. The main result of this note is the following for which we introduce some notation. Let K be a hyperbolic knot (or link) such that $S^3 \setminus K = \mathbb{H}^3 / \Gamma$, say that K has *nonintegral trace* (resp. *integral trace*) if Γ contains an element whose trace is an algebraic non-integer (resp. there is no such element).

Theorem 1.1. *There are infinitely many distinct knots with nonintegral trace.*

We provide some additional context for Theorem 1.1. As far as the authors are aware this is the first infinite family of knots in S^3 that have been proved to have nonintegral trace. Some examples of such knots were already known from the knot tables [24] (e.g., 10_{98} and 10_{99} as can be readily checked with SnapPy [10] or Snap [8]). Furthermore, Snap [8] identifies 21 examples of knots through 12 crossings that have nonintegral trace. In Section 5 we extend this list, providing 170 examples of knots up through 12 crossings that we are able to confirm have nonintegral trace.

In the case of links, it was shown in [22, Theorems 5.1 & 6.3] that there are infinitely many hyperbolic links (which have many components) with nonintegral trace, and in [7] it was shown that there exist infinitely many 2 component hyperbolic links that have nonintegral trace. The paper [28] provides a method to construct 1-cusped manifolds $\mathbb{H}^3 / \Gamma$ for which Γ has nonintegral trace, however, it seems to difficult to control the topology of this manifold and arrange that the construction produces infinitely many manifolds homeomorphic to knot complements in S^3

2. The basic construction

Our basic construction is easy to explain. First, for convenience, we recall the following interpretation of the linking number (see [24, p. 132]). Let $L = J \cup K \subset S^3$ be a 2-component link, and let $[\gamma]$ denote a generator of $H_1(S^3 \setminus J, \mathbb{Z}) \cong \mathbb{Z}$. The homology class $[K] \in H_1(S^3 \setminus J, \mathbb{Z})$ is represented by $n.[\gamma]$ for some $n \in \mathbb{Z}$, and the *linking number* of J and K is n.

Now let $L = J \cup K \subset S^3$ be a 2-component hyperbolic link with $S^3 \setminus L \cong \mathbb{H}^3 / \Gamma$, where J is the unknot and for which the linking number between J and K is 2 (after a choice of orientation of J and K). Now cyclic branched covers of S^3 branched over J are all homeomorphic to S^3. Moreover, using the definition of the linking number given above, we see that for d odd, the preimage of K in the d-fold cyclic branched cover is connected. That is to say, such d-fold cyclic branched covers of S^3 branched over J will be knot complements in S^3. For d large enough the knots will be hyperbolic as can be seen from Thurston's Dehn Surgery Theorem using the description of these branched covers as orbifold $(d, 0)$-Dehn filling on J, and subsequent passage to the appropriate d-fold cyclic cover of the orbifold.

We will also insist that there exists $\alpha \in \Gamma$ whose trace is an algebraic non-integer. As noted above, it follows that $S^3 \setminus L$ contains a closed embedded essential surface. That the knot complements constructed in the previous paragraph also contain a closed embedded essential surface follows from [16], however, it is more subtle to prove that the knots have nonintegral trace. To do this, we need to
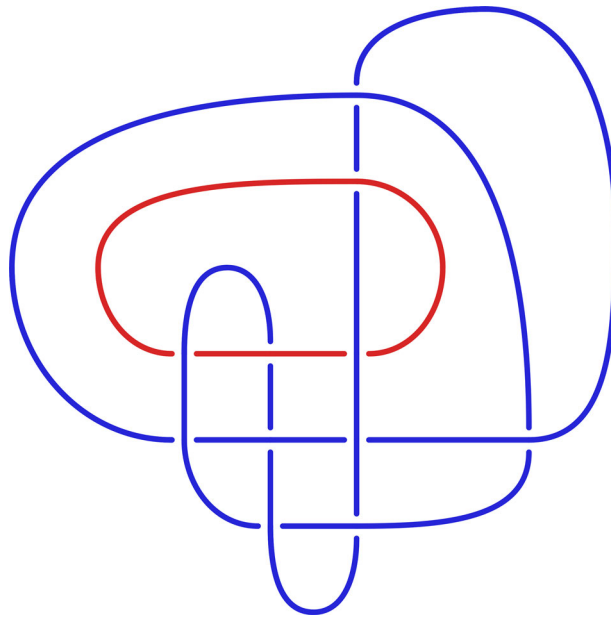

Figure 1. The link L11n106. Diagram produced in SnapPy.

analyze the behavior of $\chi_\rho(\alpha)$ on the canonical component of L. In particular, by understanding how $\chi_\rho(\alpha)$ varies on a particular subvariety of the canonical component of L we will prove that for infinitely many odd d, at those characters χ_d corresponding to $(d, 0)$-Dehn filling on J (and where the cusp corresponding to K remains a cusp), $\chi_d(\alpha)$ remains an algebraic non-integer. As is well-known, since nonintegral trace is preserved by passage to finite index subgroups (see for example [19, Corollary 3.1.4]), it follows that the knots constructed in the previous paragraph have nonintegral trace.

3. Details about *L*

The link L we use is `L11n106` from Thistlethwaite's table of 2 component links through 11 crossings [25], and shown in Figure 1. As in Section 2, J will denote the unknotted component of L, and K the knotted component of L, which in this case is the knot 7_6 of the tables of [24]. The volume of $S^3 \setminus L$ is approximately 10.666979133796239. We note that several examples were tested before the plan outlined in Section 2 was pushed through to completion (see Section 6 for a discussion of one example that failed).

In the subsections below, we gather the details about $S^3 \setminus L = \mathbb{H}^3 / \Gamma$ that will be used, together with analysis of characters. We made heavy use of Snap [8], SnapPy [10] and Mathematica [26] in our calculations.

3.1. Presentation for Γ

From SnapPy a presentation for Γ is given as follows.

```
<a,b | abbbaBAbaabABaBAbaabABabbbaBAbaabABBBAbaBAABabAbaBAABabABBBAbaBAAB=1>
```

where A and B denote the inverses of a and b respectively. Also from SnapPy meridians for J and K are given by

```
J: baabABabbbaBAABabABBBAbaBAABabbbaBA
K: ba
```

This can be checked by performing $(1, 0)$-Dehn filling on J which SnapPy shows results in a manifold homeomorphic to the complement of the knot 7_6.

Using SnapPy (or Snap) it can be checked that the trace-field of Γ is $\mathbb{Q}(\sqrt{-7})$ and that $\operatorname{tr}(a) = \pm(13 + 7\sqrt{-7})/8$ and $\operatorname{tr}(b) = \pm(17 + 3\sqrt{-7})/8$ and so both are algebraic non-integers (this can also be checked using the character variety calculations below).

3.2. Character variety calculations

Since Γ is 2-generator, we can conjugate any irreducible representation $\rho : \Gamma \to \operatorname{SL}(2, \mathbb{C})$ so that $\rho(a)$ fixes ∞ and $\rho(b)$ fixes 0. Since we are interested in those representations ρ for which the meridian of K (identified as ba in Section 3.1) continues to be parabolic, we can normalize so that $\chi_\rho(ba) = -2$ (where the minus sign is chosen so as to be consistent with the output produced by SnapPy). With this arrangement, we have

$$a \mapsto \begin{pmatrix} x & 1 \\ 0 & \frac{1}{x} \end{pmatrix} \text{ and } b \mapsto \begin{pmatrix} y & 0 \\ -xy - 2 - \frac{1}{xy} & \frac{1}{y} \end{pmatrix}$$

To handle evaluation in Mathematica of the relation on the matrices, we split it up as follows:

```
w1 = a.b.b.b.a.B.A.b.a.a.b.A.B;
w2 = a.B.A.b.a.a.b.A.B.a.b.b.b.a.B.A.b;
w3 = a.a.b.A.B.B.B.A.b.a.B.A.A.B.a.b.A.b.a;
w4 = B.A.A.B.a.b.A.B.B.B.A.b.a.B.A.A.B;
```

and evaluate

```
rel=Factor[w1.w2-Inverse[w3.w4]]
```

Setting $X = \chi_\rho(a)$ and $Y = \chi_\rho(b)$ we find that X and Y satisfies $P(X, Y) = 0$ where:

$$\begin{aligned}
P(X, Y) = {} & X^8Y + 7X^7Y^2 - 2X^7 + 21X^6Y^3 - 7X^6Y + 35X^5Y^4 - 3X^5Y^2 - 8X^5 + 35X^4Y^5 \\
& + 20X^4Y^3 - 29X^4Y + 21X^3Y^6 + 40X^3Y^4 - 39X^3Y^2 - 7X^3 + 7X^2Y^7 + 33X^2Y^5 \\
& - 23X^2Y^3 - 17X^2Y + XY^8 + 13XY^6 - 5XY^4 - 14XY^2 + X + 2Y^7 - 4Y^3
\end{aligned}$$

It is easy to check using Mathematica that $P(X, Y)$ is irreducible over $\mathbb{Q}$, and using the feature `Factor[*, Extension -> All]`, Mathematica can check that this is irreducible over $\mathbb{C}$. Indeed, our computations show that there are two subvarieties in the $\mathrm{SL}(2, \mathbb{C})$-character variety of L, where ba is kept parabolic, and the one above was identified by using the traces of a and b given at the faithful discrete representation.

Set $t = \chi_\rho(m_0)$ where m_0 is the meridian of J described above. This results in a polynomial $Q(t, X, Y)$ displayed in Section 8, and taking the resultant of $P(X, Y)$ and $Q(t, X, Y)$ to eliminate X, yields the polynomial $R(t, Y)$ displayed in Section 8 with the highest degree term as a polynomial in $\mathbb{Z}[t]$ being $16tY^{24}$. Thus, if at algebraic integer specializations of t, the polynomial $R(t, Y)$ remains irreducible, then Y is an algebraic non-integer. Note that $R(-2, Y)$ is reducible, factoring as

$$\begin{aligned}
R(-2, Y) = {} & \left(Y^9 + 15Y^8 + 104Y^7 + 435Y^6 + 1205Y^5 + 2285Y^4 + 2956Y^3 + 2506Y^2 + 1257Y + 283\right)^2 \\
& \left(2Y^2 - 5Y + 4\right)\left(4Y^2 - 17Y + 22\right)\left(4Y^2 - 11Y + 8\right)
\end{aligned}$$

with the factor corresponding to the complete structure being $4Y^2 - 17Y + 22$.

The proof of Theorem 1.1 will be completed by the following proposition, the proof of which is given in Section 4. For d odd, perform $(d, 0)$-Dehn filling on J, which amounts to setting $t = 2\cos(2\pi/d)$ in $R(t, Y)$. Now for d odd, $2\cos(2\pi/d)$ is a unit. To see this, let $\Phi_d(x)$ denote the dth cyclotomic polynomial, and let ζ_d be a primitive dth root of unity. Then $2\cos 2\pi/d = \zeta_d + 1/\zeta_d$ is a unit if and only if $\zeta_d^2 + 1$ is a unit. By [17, Lemma 2.5] this holds if and only $\Phi_d(i)$ is a unit, and this can be deduced from [6, Lemma 23] for example.

Proposition 3.1. *For infinitely many odd $d > 1$, the polynomial $R(2\cos(2\pi/d), Y)$ is irreducible over $\mathbb{Q}(\cos(2\pi/d))$.*

4. Proving irreducibility

Our goal in this section is to prove Proposition 3.1. Rather than working with the polynomial $R(t, Y)$ directly, we will instead consider the polynomial $S(X, Y) = X^8R(X + X^{-1}, Y)$ (see Section 8 for an explicit description of S). The reason for making this transformation is the following. Let $\zeta_d = \exp(2\pi i/d)$, and note that $S(\zeta_d, Y) = \zeta_d^8 R(2\cos(2\pi/d), Y)$, so $S(\zeta_d, Y)$ is irreducible in $\mathbb{Q}(\zeta_d)[Y]$ if and only if $R(2\cos(2\pi/d), Y)$ is. That $S(\zeta_d, Y)$ is irreducible in $\mathbb{Q}(\zeta_d)[Y]$ will be established using the following result.

Theorem 4.1. *[14, Corollary 1(a)] Let k be a number field and k^c the field obtained by adjoining all roots of unity to k. If $f \in k^c[X, Y]$ and $f(X^m, Y)$ is irreducible in $k^c[X, Y]$ for all positive integers $m \le \deg_Y f$, then $f(\zeta, Y)$ is irreducible in $k^c[Y]$ for all but finitely many roots of unity ζ.*

Thus, Proposition 3.1 follows immediately from Theorem 4.1 once we show that $S(X^m, Y)$ is irreducible over $\mathbb{Q}^c = \mathbb{Q}^{ab}$ for each positive integer $m \le 24$. In fact we will prove that $S(X^m, Y)$ is irreducible over $\overline{\mathbb{Q}}$ for such m; that is, $S(X^m, Y)$ is absolutely irreducible.

To accomplish this, we use [4]. Before stating the result of Bertone et al. [4] that we need, we recall the definition of the Newton polygon of a 2-variable polynomial. To that end, let $k \subset \mathbb{C}$ be a field and $f(X, Y) = \sum_{i,j} c_{i,j}X^iY^j \in k[X, Y]$. The Newton polygon of P is the convex hull in $\mathbb{R}^2$ of all points (i, j) such that $c_{i,j} \ne 0$. We call a point in the Newton polygon a *vertex* if it does not belong to the interior of any line segment in the Newton polygon. With this we have the following test for irreducibility.

Theorem 4.2. *[4, Proposition 3] Let k be a field and $f(X, Y) \in k[X, Y]$ be an irreducible polynomial. Let $\{(i_1, j_1), \ldots, (i_l, j_l)\} \subset \mathbb{Z}^2$ be the vertex set of its Newton polygon. If $\gcd(i_1, j_1, \ldots, i_l, j_l) = 1$, then $f(X, Y)$ is irreducible over $\bar{k}$.*

In our context, two things need to be established for each $m \leq 24$:
1. *$S(X^m, Y)$ is irreducible over $\mathbb{Q}$;*
2. *the Newton polygon of $S(X^m, Y)$ satisfies the conditions of Theorem 4.2.*
Proof of **1.** It can be checked quite quickly using Mathematica (for example), that $S(X^m, Y)$ is irreducible over $\mathbb{Q}$ for $m \leq 24$. However, we also supply explicit ideals I_m of $\mathbb{Z}[X, Y]$ such that the reduction of $S(X^m, Y)$ modulo I_m is an irreducible polynomial over a finite field. We include below a table of prime numbers p such that $S(X^m, Y)$ is irreducible modulo $I_m = (X - 2, p)$.

m	p	m	p	m	p
1	17	9	17	17	11
2	11	10	89	18	11
3	11	11	17	19	17
4	31	12	11	20	53
5	17	13	11	21	17
6	31	14	31	22	11
7	11	15	17	23	11
8	11	16	31	24	31

Proof of **2.** Let us first observe that the effect of replacing X with X^m is to *stretch* the Newton polygon of $S(X, Y)$ in the positive X-direction. More precisely, if (i, j) is a point in the Newton polygon (not necessarily on the boundary) of $S(X, Y)$, then (mi, j) is a point in the Newton polygon of $S(X^m, Y)$.

From Section 8, we observe that $S(X, Y)$ has a Y monomial term with coefficient 1. Moreover, further inspection of $S(X, Y)$ shows that 1 is the only power k such that Y^k has nonzero coefficient in $S(X, Y)$. Hence $(0, 1)$ is a vertex of the Newton polygon; see Figure 2.
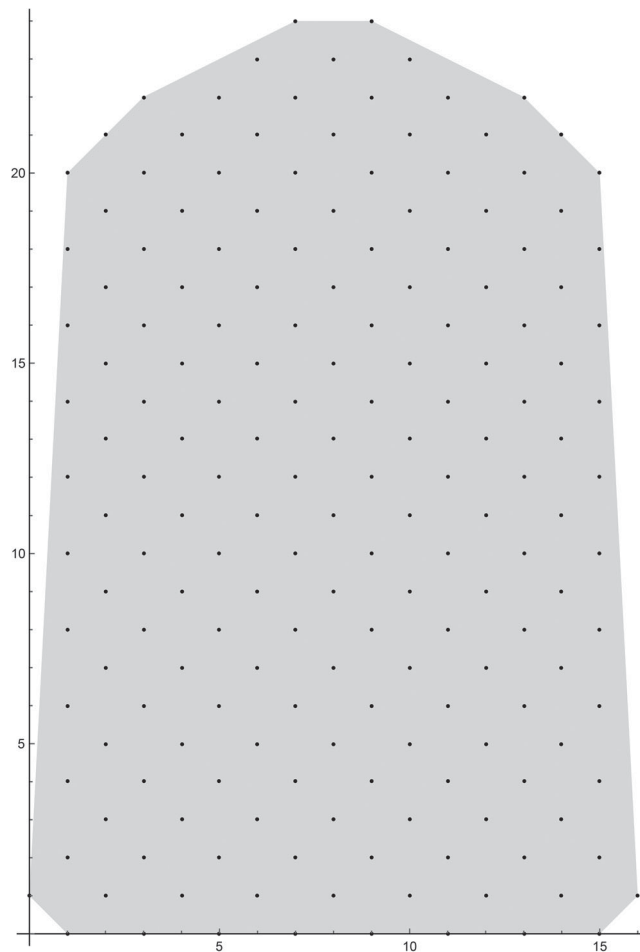

Figure 2. The Newton polygon of $S(X, Y)$ is the convex hull of the black points corresponding to nonzero coefficients of $S(X, Y)$.

In fact $(0, 1)$ will be a vertex of the Newton polygon of $S(X^m, Y)$ for all $m \geq 1$. To see this note that after replacing X with X^m, the monomial term in Y still has a coefficient 1 and will remain the only power of Y that has a nonzero coefficient; i.e. $(0, 1)$ will continue to be a vertex of the Newton polygon of $S(X^m, Y)$ for all $m \geq 1$. Thus $S(X^m, Y)$ satisfies the hypotheses of Theorem 4.2 whenever $S(X^m, Y)$ is irreducible over $\mathbb{Q}$.

With these two statements in hand, we may then conclude that $S(X^m, Y)$ is absolutely irreducible for $m \leq 24$ and hence, by Theorem 4.1 that $S(\zeta, Y)$ is irreducible over $\mathbb{Q}(\zeta)$ for all but finitely many roots of unity ζ. This, together with the discussion at the start of this section completes the proof of Proposition 3.1. $\square$

5. Knots through 12 crossings with nonintegral trace

In this section, we extend the list of Burton et al. [5] of knots with nonintegral trace through 12 crossings that we are able to confirm have nonintegral trace. As noted previously, a knot K with nonintegral trace contains a closed embedded essential surface in its complement. In [5], they show that of the 2977 knots in the census of nontrivial prime knots with ≤ 12 crossings, 1019 of these knots contain a closed embedded essential surface in their complement, and it is this list of 1019 that is our starting point.

We were able to determine whether or not traces were integral or not for 450 of them, and of those 450 knots, we determined that 170 of them have nonintegral trace. The tables were compiled using recent additions to SnapPy that, in principle, allow one to compute exactly elements of Γ whose traces generate the trace-field $\mathbb{Q}(\operatorname{tr} \Gamma)$. Indeed, as is well known (see [19, Chapter 3.5] for example), the trace of every element in Γ is an integer polynomial in the traces of any finite generating set of Γ together with a finite number of products of the generators, and so these traces suffice to certify nonintegral trace in the sense described below.

We capped the number of digits that the algebraic numbers were computed to as well as their degree (at 50) to allow for reasonable runtime. For those knots that we were unable to decide integral or nonintegral, one needs additional precision or to raise the degree.

In the tables that follow we list the 170 knots with nonintegral trace, together with rational primes p that *certify* non-integrality. By this we mean that if $S^3 \setminus K = \mathbb{H}^3/\Gamma$, then there exists $\alpha \in \Gamma$ with $\operatorname{tr}(\alpha) = r/s \in \mathbb{Q}(\operatorname{tr} \Gamma)$ and a prime ideal $\mathcal{P} \subset \mathbb{Q}(\operatorname{tr} \Gamma)$ with $\mathcal{P}| < s >$ of norm p^a for some integer $a > 0$. In this notation, for the knots constructed in the proof of Theorem 1.1, non-integrality was certified by $p = 2$.

129 *knots with* $p = 2$:

9_{29}	9_{38}	10_{96}	10_{97}	10_{99}	11a38	11a102	11a123	11a124
11a126	11a173	11a232	11a244	11a291	11a292	11a293	11a294	11a346
11a347	11a353	11a354	11n65	11n66	11n68	11n69	11n97	11n99
11n156	12a66	12a74	12a100	12a150	12a156	12a163	12a199	12a207
12a231	12a244	12a245	12a260	12a311	12a331	12a396	12a414	12a435
12a491	12a493	12a494	12a634	12a647	12a702	12a706	12a708	12a771
12a798	12a818	12a845	12a847	12a853	12a862	12a873	12a886	12a939
12a940	12a1059	12a1062	12a1097	12a1124	12a1156	12a1173	12a1261	12a1266
12a1270	12a1288	12n49	12n50	12n51	12n52	12n53	12n100	12n101
12n102	12n140	12n141	12n156	12n158	12n175	12n176	12n201	12n202
12n203	12n204	12n211	12n245	12n246	12n247	12n253	12n254	12n257
12n258	12n259	12n265	12n266	12n267	12n268	12n269	12n270	12n329
12n330	12n331	12n364	12n365	12n423	12n484	12n494	12n495	12n496
12n518	12n600	12n601	12n602	12n605	12n665	12n672	12n690	12n694
12n695	12n697	12n888						

24 *knots with* $p = 3$:

10_{90}	10_{93}	10_{122}	11a288	12a389	12a430	12a868	12a1043	12a1105
12a1109	12a1246	12n193	12n194	12n195	12n196	12n215	12n216	12n217
12n454	12n456	12n689	12n840	12n879	12n886			

17 *remaining cases*:

Knot	Primes	Knot	Primes	Knot	Primes
10_{98}	2,3	12a567	23	12n264	7
11a132	2,3	12a701	2,5	12n440	2,3
11a323	5	12a1117	13	12n508	2,3
12a348	2,3	12a1203	7	12n604	2,3
12a466	7	12a1205	17	12n868	5
12a483	7	12n256	7		

6. Remarks on nonintegral trace

In this section, we gather together some comments about nonintegral trace, how it persists in certain Dehn fillings and disappears in others. In particular, the example of the link given in Section 6.2 stands in contrast to the link L we use in the proof of Theorem 1.1, in that, as described in Section 6.2, non-integrality does not persist in $(d, 0)$-Dehn filling in this case. This clearly needs to be better understood.

6.1. Some remarks on $S^3 \setminus L$

One closed embedded essential surface in the complement of the link L can be constructed from the essential tangle decomposition shown in Figure 3. The 4-punctured sphere S shown in Figure 3 is incompressible, and tubing S provides a closed embedded essential surface F.

Note that $(1, n)$-Dehn filling on J compresses the surface F described above, since the result of $(1, n)$-Dehn filling on J produces a rational tangle on the filled side of S. Although we cannot prove compressibility of all closed embedded essential surfaces in the complement of L upon the result of $(1, n)$-Dehn filling on J, we expect this to be the case, and provide some evidence for this below.

The knot 7_6 is a 2-bridge knot, and hence its complement does not contain a closed embedded essential surface (see for example [16]). Using SnapPy, we identified that $(-1, 1)$, $(1, 1)$, $(-1, 2)$, and $(1, 2)$ Dehn fillings on the component J produce manifolds homeomorphic to the complements of 9_{43}, 10_{129}, $K11n57$, and $K12n238$, respectively, all of which are again manifolds that do not contain a closed embedded essential surface (as can be checked using [5] or KnotInfo [18]). Since the Dehn fillings described above do not contain a closed embedded essential surface, any closed embedded essential surface contained in $S^3 \setminus L$ must compress in these Dehn fillings. It follows from Culler et al. [9] and Wu [27] that any closed embedded essential surface in $S^3 \setminus L$ must contain an essential simple closed curve that is isotopic to the longitude of J.

From the above discussion, the knots 7_6, 9_{43}, 10_{129}, $K11n57$ and $K12n238$ all have integral trace. In particular, $t = \chi_\rho(m_0)$ as in Section 3.2, is an algebraic integer, as is the solution for Y obtained from $R(t, Y) = 0$ in these cases. Hence, at these values of t, the polynomial $R(t, Y)$ must be reducible. We expect this to be the case more generally for $(1, n)$ Dehn filling on J.
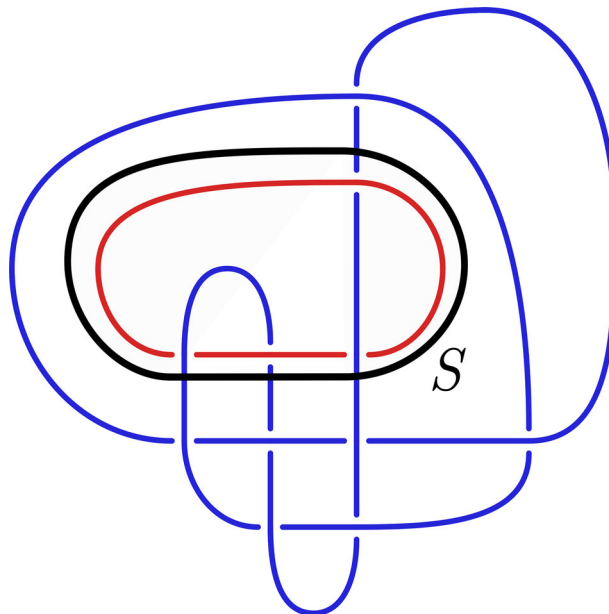

Figure 3. The surface S shown in black is an incompressible 4-punctured sphere.

6.2. Another link

Another 2 component link with an unknotted component, with linking number 2 between the two components and has nonintegral trace is the link `L11n71` from Thistlethwaite's table [25]. Executing the same plan as we described above leads to analogous polynomial $R_1(t, Y)$ shown below:

$$
\begin{aligned}
R_1(t, Y) = {}& 32768t^5 + t^3 Y^{18} - 393216t^3 + \left(3t^5 - 72t^3 + 210t\right)Y^{16} + \left(-22t^5 + 792t^3 - 2734t\right)Y^{14} \\
& + \left(104t^5 - 5928t^3 + 25240t\right)Y^{12} + \left(-320t^5 + 30240t^3 - 151360t\right)Y^{10} + \left(256t^5\right. \\
& \left. - 105728t^3 + 660224t\right)Y^8 + \left(3072t^5 + 195584t^3 - 1746944t\right)Y^6 + \left(-4096t^5 - 192512t^3\right. \\
& \left. + 3059712t\right)Y^4 + \left(-16384t^5 + 245760t^3 - 3776512t\right)Y^2 + \left(3t^4 - 25t^2\right)Y^{17} + \left(456t^4\right. \\
& \left. - 5968t^2 + 4888\right)Y^{13} + \left(-2448t^4 + 41104t^2 - 40752\right)Y^{11} + \left(9024t^4 - 201664t^2\right. \\
& \left. + 223936\right)Y^9 + \left(-15872t^4 + 649216t^2 - 881408\right)Y^7 + \left(-10240t^4 - 1182720t^2\right. \\
& \left. + 1587200\right)Y^5 + \left(73728t^4 + 946176t^2 - 479232\right)Y^3 + \left(-65536t^4 - 163840t^2\right. \\
& \left. - 1638400\right)Y + \left(t^6 - 69t^4 + 650t^2 - 593\right)Y^{15} + 3276800t.
\end{aligned}
$$

with leading term $t^3 Y^{18}$. When $t = 2$ (i.e., at the faithful discrete representation) this factors as

$$
\left(Y^3 + 2Y^2 - 4Y - 16\right)^2 \left(Y^4 - 2Y^3 - 4Y^2 + 8Y + 16\right)^2 \left(8Y^4 - 52Y^3 + 132Y^2 - 153Y + 68\right)
$$

with the term $\left(8Y^4 - 52Y^3 + 132Y^2 - 153Y + 68\right)$ corresponding to the faithful discrete representation.

As noted in Section 4, for d odd, $2\cos 2\pi/d$ is always a unit. Thus specializing the polynomial $R_1(t, Y)$ at such $t = 2\cos 2\pi/d$ shows that Y is an algebraic integer for all odd $d \geq 2$.

The knotted component of `L11n71` is the knot 7_4 which is a 2-bridge knot. Repeating the analysis that we did on L, we identified that $(-1, 1)$, $(1, 1)$, $(-1, 2)$ and $(1, 2)$ Dehn fillings on the unknotted component produce manifolds homeomorphic to the complements of 7_3, 10_{130}, 10_{128} and $K12n723$ respectively, which are again all manifolds that do not contain a closed embedded essential surface (as can be checked using [5] or KnotInfo [18]). Hence these knots have integral trace. Moreover, as with L, any closed embedded essential surface contained in the complement of `L11n71` must compress in these fillings, and as before it follows from Culler et al. [9] and Wu [27] that any closed embedded essential surface in the complement of `L11n71` must contain an essential simple closed curve that is isotopic to the longitude of the unknotted component.

As with L, from the link diagram shown in Thistlethwaite's table [25], one sees an essential tangle decomposition of `L11n71`, which can be tubed to construct a closed embedded essential surface in the complement of the link `L11n71`.

6.3. The manifold m137

The manifold $m137$ (denoted M in what follows) of the SnapPy census is a knot complement in $S^2 \times S^1$, and has been of some interest (see [11] and [15]). Moreover, it is the "smallest" cusped hyperbolic 3-manifold, we know of that has nonintegral trace. From SnapPy, a presentation of $\pi_1(M)$ is `<a,b |aaabbABBBAbb=1>`, with the faithful discrete representation being given by:

$$
a \mapsto \begin{pmatrix} -\frac{3}{2} + \frac{i}{2} & 1 \\ -1 & 0 \end{pmatrix} \text{ and } b \mapsto \begin{pmatrix} 0 & 1 \\ -1 & -\frac{1}{2} - \frac{i}{2} \end{pmatrix}.
$$

A peripheral system for M is given by $\{a^{-1}b^2 a^4 b^2, (ba)^{-1}\}$. Note that $(0, 1)$ Dehn filling gives $S^2 \times S^1$. Following Gao [15], set $\lambda = (ba)^{-1}$, then $\pi_1(M)$ can be generated by $\{b, \lambda\}$ and using this, a description for the canonical component of M is given in [15] as the curve in $\mathbb{C}^2$ obtained as the vanishing set of the polynomial:

$$
P(s, t) = (-2 - 3s + s^3)t^4 + (4 + 4s - s^2 - s^3)t^2 - 1,
$$

where $s = \chi_\rho(\lambda)$, $t = \chi_\rho(b)$ and $\chi_\rho(b\lambda) = t - \frac{1}{t(s+1)}$. Note that $(-2 - 3s + s^3) = (s + 1)^2(s - 2)$ and $(4 + 4s - s^2 - s^3) = (s + 1)(s + 2)(s - 2)$. Thus, understanding the behavior of $t = \chi_\rho(b)$ (i.e. integral versus non-integral) is reduced to understanding when $(s + 1)$ and $(s - 2)$ are units in the number fields arising from Dehn filling representations.

For example, if we consider $(0, d)$ Dehn fillings with d odd, we are led to consideration of when $(2\cos(2\pi/d) + 1)$ and $(2\cos(2\pi/d) - 2)$ are and are not units. For d even similar statements hold for $(2\cos(2\pi/2d) + 1)$ and $(2\cos(2\pi/2d) - 2)$. For ease of exposition we will assume that d is odd.

Now $(2\cos(2\pi/d) - 2)$ is never a unit for d a power of a prime (resp. is a unit when d is not a power of a prime). To see this note that: $(2\cos(2\pi/d) - 2) = \zeta_d + 1/\zeta_d - 2 = (\zeta_d - 1)^2/\zeta_d$, where ζ_d is a primitive dth root of unity. As above, let $\Phi_d(x)$ denote the d-th cyclotomic polynomial, then $\zeta_d - 1$ is a unit if and only if $\Phi_d(1) = \pm 1$ (see for example [17, Lemma 2.5]). It is a well-known property of cyclotomic polynomials that this happens if and only d is not a power of a prime. Similarly, when $(2\cos(2\pi/d) + 1)$ is a unit reduces to understanding when $\zeta_d^2 + \zeta_d + 1$ is a unit, which by [17, Lemma 2.5] holds if and only if $\Phi_d(\omega)$ is a unit where ω is a primitive cube root of unity.
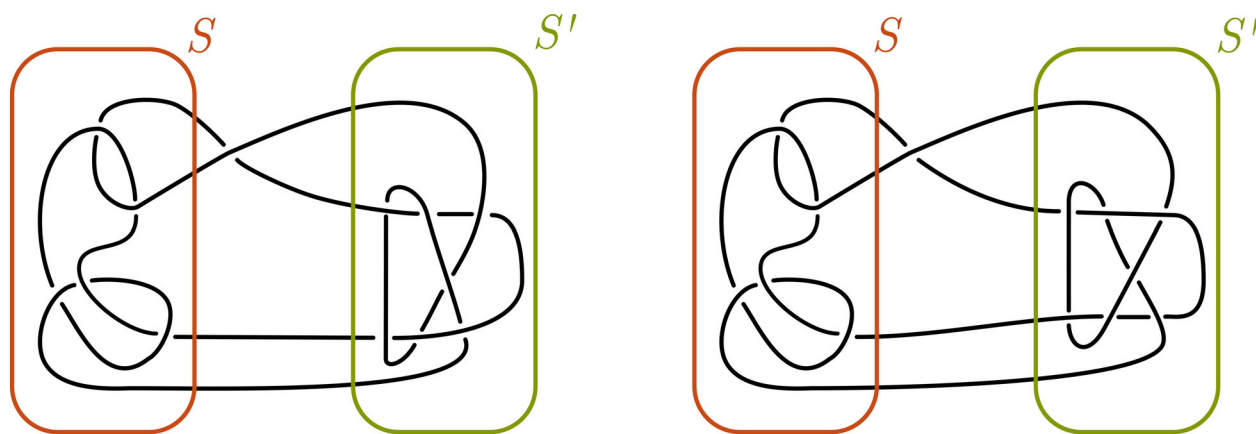
Figure 4. The knot `12n253` on the left and `12n254` on the right. The essential 4-punctured spheres, S and S', provide an essential tangle decomposition for each knot.

We have not analyzed all of this carefully, but experiments seem to support that $(0, d)$ Dehn fillings have integral trace (so modulo irreducibility concerns both the above terms are units) when $d = 10k$, $k \geq 1$. We also found that $(0, 14)$ has integral trace.

Experiments also suggest that many other Dehn fillings have integral traces; for example it seems that for n an integer, the family of $(1, n)$ Dehn fillings have integral trace. In particular, we checked this holds for integers $n \in [-7, -3] \cup [2, 6]$ and so at such Dehn fillings s and t will be algebraic integers. Hence in these cases, from the expression for $P(s, t)$ (modulo irreducibility concerns), we deduce that $(s + 1)$ and $(s - 2)$ must be units in the number fields constructed by these Dehn fillings.

We also note that using Culler et al. [9] and Wu [27] any closed embedded essential surface in M must contain an essential simple closed curve that is isotopic to λ. To see this, as noted above, $(0, 1)$ Dehn filling produces $S^2 \times S^1$, any closed embedded essential surface in M must compress in this filling. Moreover, SnapPy shows that $(-1, 3)$, $(-1, 4)$, $(-1, 5)$, $(1, 2)$, $(1, 3)$ and $(1, 5)$ are all hyperbolic, all have volume < 3 and have a shortest closed geodesic of length > 0.3. Hence using the list of small volume Haken manifolds from [12] all of these manifolds are non-Haken hyperbolic 3-manifolds. Hence any closed embedded essential surface in M must compress in these fillings. In addition, $(-1, 1)$ Dehn filling results in a small Seifert fibered space, and so again, any closed embedded essential surface in M must compress in this filling.

From Culler et al. [9] and Wu [27], the only way that all of these compressions can happen is that any closed embedded essential surface in M must contain an essential simple closed curve that is isotopic to λ.

7. Questions and comments

We gather together some questions raised by this work, as well as some comments.

Existence of accidental parabolic elements: In the two examples of link complements considered in this paper, as well as the example of $m137$, the closed embedded essential surfaces in the these manifolds carried essential curves that were isotopic to essential simple curves on a boundary torus, these are examples of *accidental parabolic elements* in the surface group. As we now describe, this also holds for all of the knots listed in Section 5.

For the alternating knots listed in Section 5, this follows from [20], for which the accidental parabolic is a meridian. As was pointed out to us by J. Howie, all the non-alternating knots listed in Section 5 (apart from `12n253` and `12n254`) are almost alternating, and so by [1] also have complements for which the meridian is an accidental parabolic on any closed embedded essential surface. Furthermore, Howie observed that the two remaining knots admit an essential tangle decomposition as shown below in Figure 4. Tubing the essential 4-punctured spheres S and S' shown in Figure 4 provides a closed embedded essential surface that carries an accidental parabolic which is a meridian.

Howie also pointed out to us that the knots constructed in the proof of Theorem 1.1 have complements that admit a closed embedded essential surface that carries an accidental parabolic element (again a meridian). We include his argument below.

Lemma 7.1 (Howie). *Let K_d denote the knot constructed in the proof of Theorem 1.1 via the d-fold cyclic branched cover of S^3 branched over J, and where d is assumed to be odd. Then $S^3 \setminus K_d$ contains a closed embedded essential surface for which the meridian is an accidental parabolic.*

Proof. Performing an isotopy to the link L results in the diagram shown in Figure 5.

The d-fold cyclic branched cover over J that we made use of in the proof Theorem 1.1 can be described as follows. Cut along the Seifert surface F shown in Figure 5, cyclically glue d copies of the resulting piece, and then glue a solid torus J' back in (where J' is the lift of J). Since the 4-punctured sphere S is disjoint from J and F, S will lift to d disjoint copies of itself, which we denote S', S'', etc. Similarly the ball-tangle pair (B, T) lifts to d disjoint copies of itself denoted (B', T'), (B'', T''), etc (see Figure 6). Note that since T is an essential tangle, S is incompressible to one side of (B, T).
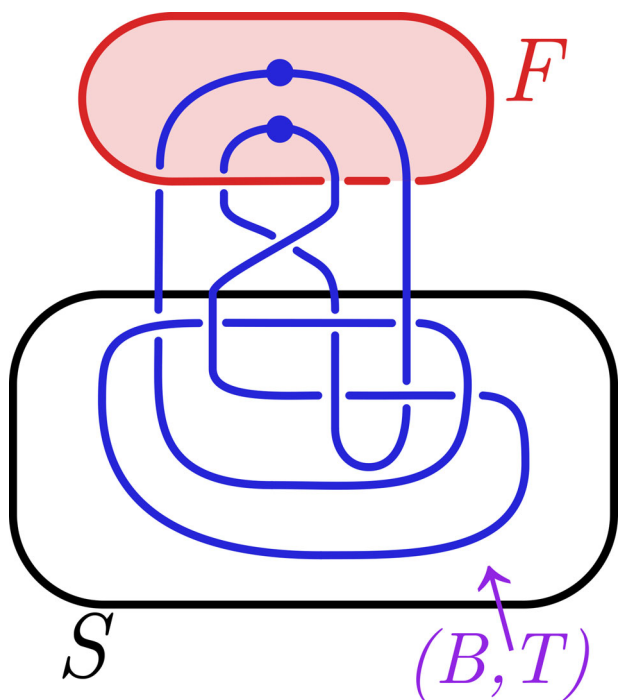
Figure 5. The link *L* after isotopy. The shaded surface *F* is a Seifert surface. The black surface *S* is a 4-punctured sphere, and (B, T) is the ball-tangle pair.
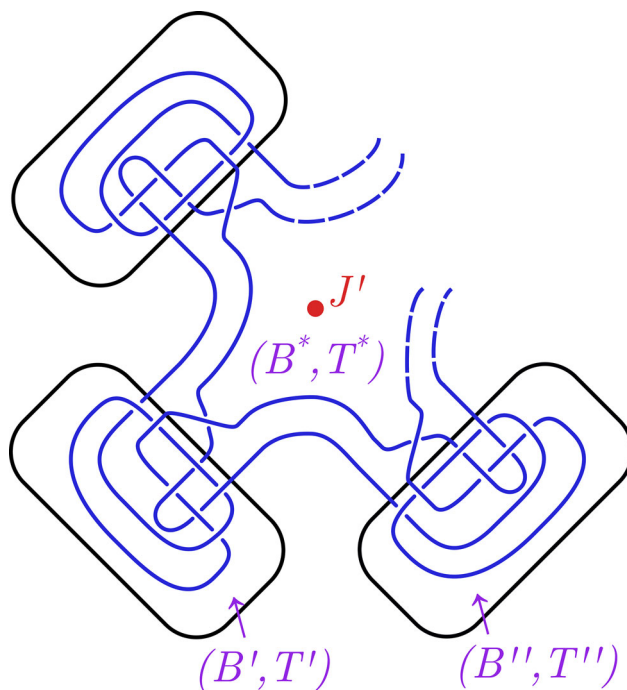

Figure 6. The *d*-fold cyclic branched cover over *J*.

Now $d \geq 3$ is odd, so S' is incompressible to one side of (B', T'), since (B', T') is simply a lift of the ball-tangle pair (B, T). It remains to show S' is incompressible on the other side. As shown in Figure 6, we write (B^*, T^*) for the ball-tangle pair on the other side of S'. Note that T^* contains no closed components. Let D be a compressing disk for S' in (B^*, T^*). Then D must separate the two strands of T^*. It follows that D must intersect S'', otherwise it would fail to separate the two strands of T'' which belong to different strands of T^*.

Now consider the intersection pattern of S'' on D. Curves which are trivial on S'' can be removed, and the only curves which remain belong to a non-empty family of parallel curves which separate pairs of points on S''. Choosing an innermost such curve determines a loop in D which bounds a disk D' say. Now D' cannot bound a disk in (B'', T'') since as above, (B'', T'') is simply a lift of the ball-tangle pair (B, T). Moreover, D' cannot bound a disk on the other side of S'', since arguing as above, D' would have to intersect S'. However,

the interior of D is disjoint from S' (since it is a compressing disk), so S' is incompressible to both sides, and therefore is essential in the complement of K_d.

We can then find at least one tubing of S' that produces a closed embedded essential surface in the complement of K_d. By construction the meridian is an accidental parabolic. □

We also note that there is a knot with nonintegral trace for which the meridian cannot be an accidental parabolic. The knot in question is `15n153789` which appeared in [13] (as an example of a "barely large knot") and contains a unique closed embedded essential surface S of genus 2. Now [13, Theorem 7.6] shows that the meridian is not a boundary slope, and so S cannot contain an essential simple closed curve isotopic to a meridian. We do not know whether this surface carries an accidental parabolic. That it has nonintegral trace can be checked using Snap or SnapPy.

Given this discussion, it seems reasonable to ask:

Question 1: *Does every knot K with nonintegral trace have a complement that contains a closed embedded essential surface containing an accidental parabolic element?*

2-**generator nonintegral knots:** A 3-manifold M is called 2-generator if $\pi_1(M)$ can be generated by two elements. A link $L \subset S^3$ is called 2-generator if $\pi_1(S^3 \setminus L)$ is 2-generator. The two links `L11n106` and `L11n71` considered in this paper, as well as the example of $m137$ are 2-generator (which greatly facilitated computation). On the other hand, none of the 170 examples listed in Section 5 appear to be "obviously" 2-generator (using SnapPy), and in a previous version of this paper we asked whether there exists a hyperbolic knot $K \subset S^3$ with nonintegral trace which is 2-generator.

The following example was pointed out to us by K. Baker and N. Hoffman. The manifold $v1980$ of the SnapPy census is homeomorphic to the complement of a Berge knot $K \subset S^3$ which they checked by SnapPy has nonintegral trace. Indeed, in the terminology of [2], K is a knot which lies on the fiber of the trefoil knot complement and so the knot arises from Berge's family VII.

Being a Berge knot, K is 2-generator, and has a Lens Space Dehn filling. In particular, it is an L-space knot in the sense of Ozsváth and Szabó [23], and so this example also answers another question from an earlier version of this paper, namely whether there exists a knot K with nonintegral trace that is an L-space knot in the sense of Ozsváth and Szabó.

Non-triviality of the Alexander polynomial: The manifold $m137$ has trivial Alexander polynomial, however it can be checked from [18] for example, that none of the 170 knots in Section 5 have trivial Alexander polynomial. Moreover, as we now show, the knots constructed in Theorem 1.1 also do not have trivial Alexander polynomial.

Proposition 7.2. *All the knots constructed in the proof of Theorem 1.1 have non-trivial Alexander polynomial.*

Proof. The Alexander polynomial of the link L used in the proof of Theorem 1.1 can be computed in SnapPy using:

```
link=snappy.Link('L11n106')
link.alexander_polynomial()
```

which gives.

$$\Delta_L(u, v) = u \left(v^5 - 2v^4 - v^3 + 3v^2 - 2v\right) - 2v^4 + 3v^3 - v^2 - 2v + 1,$$

where u is the meridian of the unknotted component J. Note that $v^5 - 2v^4 - v^3 + 3v^2 - 2v$ factors as $v(v-2)(v^3 - v + 1)$

As above, let K_d denote the knot constructed in the proof of Theorem 1.1 via the d-fold cyclic branched cover of S^3 branched over J, and where d is assumed to be odd. Using [21, Proposition 4.1 & Theorem 1] and the fact that the branch locus is the unknot, it follows that the Alexander polynomial of K_d is given by:

$$\Delta_{K_d}(u) = \prod_{i=1}^{d-1} \Delta_L(u, \zeta_d^i),$$

where ζ_d is a primitive d-th root of unity.

Note that this product produces a polynomial in u of degree $d - 1$ with leading coefficient $\prod_{i=1}^{d-1} \zeta_d^i(\zeta_d^i - 2)(\zeta_d^{i^3} - \zeta_d^i + 1)$. Neither of $(\zeta_d^i - 2)$ or $(\zeta_d^{i^3} - \zeta_d^i + 1)$ are factors of cyclotomic polynomials and so the product is never zero. Hence $\Delta_{K_d}(u) \neq 1$ as required. □

Question 2: *Does there exist a hyperbolic knot K with nonintegral trace and with trivial Alexander polynomial?*

8. Additional Mathematica output

$$Q(t, X, Y) = -t + X^{16}Y^3 + 16X^{15}Y^4 - 6X^{15}Y^2 + 120X^{14}Y^5 - 83X^{14}Y^3 + 12X^{14}Y + 560X^{13}Y^6$$

$$- 532X^{13}Y^4 + 132X^{13}Y^2 - 8X^{13} + 1820X^{12}Y^7 - 2093X^{12}Y^5 + 644X^{12}Y^3 - 44X^{12}Y$$
$$+ 4368X^{11}Y^8 - 5642X^{11}Y^6 + 1800X^{11}Y^4 + 10X^{11}Y^2 - 32X^{11} + 8008X^{10}Y^9$$
$$- 11011X^{10}Y^7 + 3036X^{10}Y^5 + 755X^{10}Y^3 - 236X^{10}Y + 11440X^9Y^{10} - 16016X^9Y^8$$
$$+ 2684X^9Y^6 + 3040X^9Y^4 - 700X^9Y^2 - 48X^9 + 12870X^8Y^{11} - 17589X^8Y^9$$
$$- 396X^8Y^7 + 6519X^8Y^5 - 939X^8Y^3 - 328X^8Y + 11440X^7Y^{12} - 14586X^7Y^{10}$$
$$- 4752X^7Y^8 + 8892X^7Y^6 - 72X^7Y^4 - 950X^7Y^2 - 32X^7 + 8008X^6Y^{13} - 9009X^6Y^{11}$$
$$- 7260X^6Y^9 + 8070X^6Y^7 + 1764X^6Y^5 - 1493X^6Y^3 - 182X^6Y + 4368X^5Y^{14}$$
$$- 4004X^5Y^{12} - 6468X^5Y^{10} + 4800X^5Y^8 + 3024X^5Y^6 - 1328X^5Y^4 - 428X^5Y^2$$
$$- 12X^5 + 1820X^4Y^{15} - 1183X^4Y^{13} - 3828X^4Y^{11} + 1690X^4Y^9 + 2670X^4Y^7$$
$$- 583X^4Y^5 - 532X^4Y^3 - 51X^4Y + 560X^3Y^{16} - 182X^3Y^{14} - 1528X^3Y^{12}$$
$$+ 202X^3Y^{10} + 1416X^3Y^8 + 2X^3Y^6 - 368X^3Y^4 - 82X^3Y^2 - 6X^3 + 120X^2Y^{17}$$
$$+ 7X^2Y^{15} - 396X^2Y^{13} - 89X^2Y^{11} + 448X^2Y^9 + 125X^2Y^7 - 134X^2Y^5 - 61X^2Y^3$$
$$- 15X^2Y + 16XY^{18} + 8XY^{16} - 60XY^{14} - 40XY^{12} + 76XY^{10} + 52XY^8 - 20XY^6$$
$$- 20XY^4 - 12XY^2 + Y^{19} + Y^{17} - 4Y^{15} - 5Y^{13} + 5Y^{11} + 7Y^9 - 2Y^5 - 3Y^3 + Y.$$

$$R(t, Y) = 669124t - 2t^7 - 498002t^5 - 5223073t^3 - 16tY^{24} + \left(120t^2 + 176\right)Y^{23} + \left(-t^5 - 344t^3\right.$$
$$\left.- 1595t\right)Y^{22} + \left(-t^7 - 265t^5 - 8323t^3 - 5017t\right)Y^{20} + \left(31t^7 - 820t^5 + 45501t^3\right.$$
$$\left.+ 26034t\right)Y^{18} + \left(-428t^7 + 34065t^5 - 60100t^3 - 223825t\right)Y^{16} + \left(3393t^7 - 229701t^5\right.$$
$$\left.- 1671221t^3 - 1389221t\right)Y^{14} + \left(-16709t^7 + 392665t^5 + 4196073t^3 + 3978713t\right)Y^{12}$$
$$+ \left(51769t^7 + 613384t^5 + 1570051t^3 + 257774t\right)Y^{10} + \left(-97592t^7 - 3180386t^5\right.$$
$$\left.- 27592720t^3 - 28733690t\right)Y^8 + \left(102474t^7 + 3256419t^5 + 42551766t^3 + 53431661t\right)Y^6$$
$$+ \left(-49677t^7 + 1658479t^5 - 6346815t^3 - 21240713t\right)Y^4 + \left(6945t^7 - 5819870t^5\right.$$
$$\left.- 50037327t^3 - 50675755t\right)Y^2 + \left(2t^6 + 466t^4 + 5400t^2 + 1265\right)Y^{21} + \left(8t^6 + 5340t^4\right.$$
$$\left.- 4891t^2 - 551\right)Y^{19} + \left(246t^6 - 65918t^4 - 71499t^2 + 10156\right)Y^{17} + \left(-8510t^6 + 292550t^4\right.$$
$$\left.+ 1114568t^2 + 263159\right)Y^{15} + \left(62972t^6 + 480016t^4 + 532043t^2 - 387\right)Y^{13} + \left(-184968t^6\right.$$
$$\left.- 4075296t^4 - 11015955t^2 - 1827985\right)Y^{11} + \left(148666t^6 + 7363350t^4 + 27163139t^2\right.$$
$$\left.+ 4743016\right)Y^9 + \left(389244t^6 + 2024132t^4 - 5822600t^2 + 2654010\right)Y^7 + \left(-959338t^6\right.$$
$$\left.- 19599946t^4 - 57150066t^2 - 22718115\right)Y^5 + \left(659693t^6 + 19149660t^4 + 77616992t^2\right.$$
$$\left.+ 31164769\right)Y^3 + \left(t^8 + 235110t^6 + 11747029t^4 + 26741431t^2 - 669124\right)Y$$

As a check, Mathematica shows that $R(-2, (17 + 3\sqrt{-7})/8) = 0$ (i.e. at the faithful discrete representation).

$$S(X, Y) = \left(-16X^9 - 16X^7\right)Y^{24} + \left(120X^{10} + 416X^8 + 120X^6\right)Y^{23}$$
$$+ \left(-X^{13} - 349X^{11} - 2637X^9 - 2637X^7 - 349X^5 - X^3\right)Y^{22}$$
$$+ \left(2X^{14} + 478X^{12} + 7294X^{10} + 14901X^8 + 7294X^6 + 478X^4 + 2X^2\right)Y^{21}$$
$$+ \left(-X^{15} - 272X^{13} - 9669X^{11} - 32671X^9 - 32671X^7 - 9669X^5 - 272X^3 - X\right)Y^{20}$$
$$+ \left(8X^{14} + 5388X^{12} + 16589X^{10} + 21867X^8 + 16589X^6 + 5388X^4 + 8X^2\right)Y^{19}$$
$$+ \left(31X^{15} - 603X^{13} + 42052X^{11} + 155422X^9 + 155422X^7 + 42052X^5\right.$$
$$\left.- 603X^3 + 31X\right)Y^{18}$$
$$+ \left(246X^{14} - 64442X^{12} - 331481X^{10} - 523430X^8 - 331481X^6 - 64442X^4 + 246X^2\right)Y^{17}$$
$$+ \left(-428X^{15} + 31069X^{13} + 101237X^{11} - 78455X^9 - 78455X^7 + 101237X^5\right.$$
$$\left.+ 31069X^3 - 428X\right)Y^{16}$$
$$+ \left(-8510X^{14} + 241490X^{12} + 2157118X^{10} + 4077395X^8 + 2157118X^6\right.$$
$$\left.+ 241490X^4 - 8510X^2\right)Y^{15}$$

$$+ \left(3393X^{15} - 205950X^{13} - 2748473X^{11} - 8581139X^9 - 8581139X^7 - 2748473X^5 \right.$$
$$\left. - 205950X^3 + 3393X\right)Y^{14}$$
$$+ \left(62972X^{14} + 857848X^{12} + 3396687X^{10} + 5203235X^8 + 3396687X^6 + 857848X^4 \right.$$
$$\left. + 62972X^2\right)Y^{13}$$
$$+ \left(-16709X^{15} + 275702X^{13} + 5808509X^{11} + 19908767X^9 + 19908767X^7 \right.$$
$$\left. + 5808509X^5 + 275702X^3 - 16709X\right)Y^{12}$$
$$+ \left(-184968X^{14} - 5185104X^{12} - 30091659X^{10} - 52011031X^8 - 30091659X^6 \right.$$
$$\left. - 5185104X^4 - 184968X^2\right)Y^{11}$$
$$+ \left(51769X^{15} + 975767X^{13} + 5724120X^{11} + 12913682X^9 + 12913682X^7 \right.$$
$$\left. + 5724120X^5 + 975767X^3 + 51769X\right)Y^{10}$$
$$+ \left(148666X^{14} + 8255346X^{12} + 58846529X^{10} + 106222714X^8 + 58846529X^6 \right.$$
$$\left. + 8255346X^4 + 148666X^2\right)Y^9$$
$$+ \left(-97592X^{15} - 3863530X^{13} - 45544082X^{11} - 146731430X^9 \right.$$
$$\left. - 146731430X^7 - 45544082X^5 - 3863530X^3 - 97592X\right)Y^8$$
$$+ \left(389244X^{14} + 4359596X^{12} + 8112588X^{10} + 10938482X^8 + 8112588X^6 + 4359596X^4 \right.$$
$$\left. + 389244X^2\right)Y^7$$
$$+ \left(102474X^{15} + 3973737X^{13} + 60985815X^{11} + 217237739X^9 + 217237739X^7 \right.$$
$$\left. + 60985815X^5 + 3973737X^3 + 102474X\right)Y^6$$
$$+ \left(-959338X^{14} - 25355974X^{12} - 149939920X^{10} - 273804683X^8 - 149939920X^6 \right.$$
$$\left. - 25355974X^4 - 959338X^2\right)Y^5$$
$$+ \left(-49677X^{15} + 1310740X^{13} + 902363X^{11} - 25435063X^9 - 25435063X^7 + 902363X^5 \right.$$
$$\left. + 1310740X^3 - 49677X\right)Y^4$$
$$+ \left(659693X^{14} + 23107818X^{12} + 164111027X^{10} + 314490573X^8 + 164111027X^6 \right.$$
$$\left. + 23107818X^4 + 659693X^2\right)Y^3$$
$$+ \left(6945X^{15} - 5771255X^{13} - 78990832X^{11} - 258743361X^9 - 258743361X^7 \right.$$
$$\left. - 78990832X^5 - 5771255X^3 + 6945X\right)Y^2$$
$$+ \left(X^{16} + 235118X^{14} + 13157717X^{12} + 77256253X^{10} + 127998182X^8 + 77256253X^6 \right.$$
$$\left. + 13157717X^4 + 235118X^2 + 1\right)Y$$
$$- 2X^{15} - 498016X^{13} - 7713125X^{11} - 19980185X^9 - 19980185X^7 - 7713125X^5$$
$$- 498016X^3 - 2X$$

Acknowledgments

Declaration of Interest

Funding

References

[1] Adams, C. C., Brock, J. F., Comar, T .D., Faigin, K. A., Huston, A. M., Joseph, A. M., Pesikoff, D. (1992). Almost alternating links. *Topol. Appl.* 46: 151–165.

[2] Baker, K. (2004). Knots on once-punctured torus fibers. Ph.D thesis, U.T. Austin.

[3] Bass, H. (1984). *Finitely Generated Subgroups of* GL$_2$, The Smith conjecture (New York, 1979), 127–136, Pure Appl. Math., Vol. 112, Orlando, FL: Academic Press.

[4] Bertone, C., Chéze, G., Galligo, A. (2010). Modular Las Vegas algorithms for polynomial absolute factorization. *J. Symbolic Comput.* 45: 1280–1295.

[5] Burton, B. A., Coward, A., Tillmann, S. (2013). Computing closed essential surfaces in knot complements. In *Proceedings of the Twenty-Ninth Annual Symposium on Computational Geometry (SoCG '13)*, New York: ACM, 405–414.

[6] Bartłomiej, B., Herrera-Poyatos, A., Moree, P. (2018). Cyclotomic polynomials at roots of unity. *Acta Arith.* 184: 215–230.

[7] Chesebro, E., DeBlois, J. (2014). Algebraic invariants, mutation, and commensurability of link complement. *Pacific J. Math.* 267: 341–398.

[8] Coulsen, D., Goodman, O. A., Hodgson, C. D., Neumann, W. D. (2000). Computing arithmetic invariants of 3-manifolds. *Experiment. Math.* 9: 127–152.

[9] Culler, M., Gordon, C. McA., Luecke, J., Shalen, P. B. (1987). Dehn surgery on knots. *Ann Math.* 125: 237–300.

[10] Culler, M., Dunfield, N. M., Goerner, M., Weeks, J. R. SnapPy, a computer program for studying the geometry and topology of 3-manifolds. Available at: http://snappy.computop.org.

[11] Dunfield, N. M. (1999). Examples of non-trivial roots of unity at ideal points of hyperbolic 3-manifolds. *Topology* 38: 457–465.

[12] Dunfield, N. M. (1999). *Which small volume hyperbolic 3-manifolds are Haken?* Slides from a talk at University of Warwick 1999. Available at: https://faculty.math.illinois.edu/~nmd/slides/haken_slides.pdf.

[13] Dunfield, N. M., Garoufalidis, S., Rubinstein, J. H. *Counting essential surfaces in 3-manifolds*. Available at: arXiv:2007.10053.

[14] Dvornicich, R., Zannier, U. (2007). Cyclotomic Diophantine problems (Hilbert irreducibility and invariant sets for polynomial maps). *Duke Math. J.* 139: 527–554.

[15] Gao, X. (2017). Non-L-space integral homology 3-spheres with no nice orderings. *Algebr. Geom. Topol.* 17: 2511–2522.

[16] Gordon, C. McA., Litherland, R. A. (1984). *Incompressible Surfaces in Branched Covers*, The Smith conjecture (New York, 1979), 139–152, Pure Appl. Math., 112, Orlando, FL: Academic Press.

[17] Lenstra, H. W. Jr, (1977). Euclidean number fields of large degree. *Invent. Math.* 38: 237–254.

[18] Livingston, C., Moore, A. H. (2020). KnotInfo: Table of Knot Invariants, Available at: http://www.indiana.edu/~knotinfo, July.

[19] Maclachlan, C., Reid, A. W. (2003). *The Arithmetic of Hyperbolic 3-Manifolds*, Graduate Texts in Math. Vol. 219. New York: Springer-Verlag.

[20] Menasco, W. (1984). Closed incompressible surfaces in alternating knot and link complements. *Topology* 23: 37–44.

[21] Murasugi, K. (1971). On periodic knots. *Comment. Math. Helv.* 46: 162–174.

[22] Neumann, W. D., Reid, A. W. (1992). *Arithmetic of Hyperbolic Manifolds*. In Topology '90 (Columbus, OH, 1990), 273–310, Ohio State Univ. Math. Res. Inst. Publ., Vol. 1, Berlin: de Gruyter .

[23] Ozsváth, P., Szabó, Z. (2005). On knot Floer homology and lens space surgeries. *Topology* 44: 1281–1300.

[24] Rolfsen, D. (1976). *Knots and Links*. Berkeley CA: Publish or Perish.

[25] *The Thistlethwaite Link Table*. Available at: http://katlas.math.toronto.edu/wiki/The_Thistlethwaite_Link_Table.

[26] Wolfram Research, Inc., (2017). *Mathematica*, Version 11.2. Champaign, IL.

[27] Wu, Y-Q. (1992). Incompressibility of surfaces in surgered 3-manifolds. *Topology* 31: 271–279.

[28] Zhang, X. (2006). The A-polynomial n-tuple of a link and hyperbolic 3-manifolds with non-integral traces. *J. Knot Theory Ramificat.* 15: 279-287.